Magnetic nature of superconductivity in doped cuprates

Shiping Feng, Tianxing Ma, and Huaiming Guo
Department of Physics, Beijing Normal University, Beijing 100875, China

Within the kinetic energy driven superconducting mechanism, the magnetic nature of cuprate superconductors is discussed. It is shown that the superconducting state is controlled by both charge carrier gap function and quasiparticle coherent weight. This quasiparticle coherent weight grows linearly with the hole doping concentration in the underdoped and optimally doped regimes, and then decreases with doping in the overdoped regime, which leads to that the maximal superconducting transition temperature occurs around the optimal doping, and then decreases in both underdoped and overdoped regimes. Within this framework, we calculate the dynamical spin structure factor of cuprate superconductors, and reproduce all main features of inelastic neutron scattering experiments, including the energy dependence of the incommensurate magnetic scattering at both low and high energies and commensurate resonance at intermediate energy.

74.20.Mn, 74.25.Ha, 74.62.Dh

I. INTRODUCTION

The interplay between the strong electron correlation and superconductivity is one of the most important problems raised by the discovery of cuprate superconductors[1]. After intensive investigations over more than a decade, it has become clear that the strong electron correlation in doped cuprates plays a crucial role not only for the unusual normal-state behavior but also for the superconducting (SC) mechanism[1–3]. The parent compound of cuprates superconductors is a Mott insulator with the antiferromagnetic (AF) long-range order (AFLRO), then changing the carrier concentration by ionic substitution or increasing the oxygen content turns these compounds into the SC-state leaving the AF short-range correlation (AFSRC) still intact[4]. As a function of the hole doping concentration, the SC transition temperature reaches a maximum in the optimal doping, and then decreases in both underdoped and overdoped regimes[5]. Moreover, this SC transition temperature is dependence of both charge carrier gap parameter and quasiparticle coherent weight[6], which strongly suggests that the quasiparticle coherence plays an important role in superconductivity.

By virtue of systematic studies using the nuclear magnetic resonance, and muon spin rotation techniques, particularly the inelastic neutron scattering, the doping and energy dependent magnetic excitations in doped cuprates in the SC-state have been well established: (a) at low energy, the incommensurate (IC) magnetic scattering peaks are shifted from the AF wave vector $[\pi,\pi]$ to four points $[(1\pm\delta)\pi,\pi]$ and $[\pi,(1\pm\delta)\pi]$ (in units of inverse lattice constant) with δ as the incommensurability parameter[7–9]; (b) then with increasing energy these IC magnetic scattering peaks are converged on the commensurate $[\pi,\pi]$ resonance peak at intermediate energy[7,10–12]; and (c) well above this resonance energy, the continuum of magnetic excitations peaked at IC positions in the diagonal direction are oberved[13–15]. It has been emphasized that the geometry of these IC magnetic excitations is two-dimensional[16,13]. Although some of these magnetic properties have been observed in the normal-state, these IC magnetic scattering and commensurate resonance are the main new feature that appears into the SC-state. Moreover, AFSRC coexists with the SC-state in the whole SC regime[9], and the unusual magnetic excitations at high energy have energies greater than the SC pairing energy, are present at the SC transition temperature, and have spectral weight far exceeding that of the resonance[13,14]. These provide a clear link between the charge carrier pairing mechanism and magnetic excitations in cuprate superconductors.

Recently, we[17] have discussed the kinetic energy driven SC mechanism in doped cuprates based on the charge-spin separation (CSS) fermion-spin theory[18], where the dressed holons interact occurring directly through the kinetic energy by exchanging dressed spin excitations, leading to a net attractive force between dressed holons, then the electron Cooper pairs originating from the dressed holon pairing state are due to the charge-spin recombination, and their condensation reveals the SC ground-state. The SC transition temperature is proportional to the hole doping concentration in the underdoped regime. However, an obvious weakness is that the SC transition temperature is too high, and not suppressed in the overdoped regime[17]. In this paper, we study the magnetic nature of the kinetic energy superconductivity in doped cuprates along with this line. A short version of this work was published earlier[19]. One of our main results is that the SC transition temperature is suppressed to low temperatures by considering the quasiparticle coherence, and therefore the SC transition temperature is controlled by both charge carrier gap function and quasiparticle coherent weight. This quasiparticle coherent weight is closely related to the dressed holon self-energy from the dressed spin pair bubble, and grows linearly with increasing doping in the underdoped and optimally doped regimes, then decreases with increasing doping in the overdoped regime, which leads to that the maximal SC transition temperature occurs around the optimal doping, and then decreases in both underdoped and overdoped regimes. Within this SC mechanism, we give a theoretical explanation of inelastic neutron scattering ex-

periments on cuprate superconductors[7,10–15] in terms of the collective mode in the dressed holon particle-particle channel.

The paper is organized as follows. The interplay between the quasiparticle coherence and superconductivity is discussed in Sec. II. In Sec. III, we calculate explicitly the dynamical spin structure factor of cuprate superconductors, and reproduce all main features found in experiments in the SC-state[7–15], including the energy dependence of the IC magnetic scattering at both low and high energies and commensurate $[\pi,\pi]$ resonance at intermediate energy. Sec. IV is devoted to a summary and discussions.

II. INTERPLAY BETWEEN THE QUASIPARTICLE COHERENCE AND SUPERCONDUCTIVITY

In doped cuprates, the single common feature is the presence of the two-dimensional CuO_2 plane[4], it is believed that the relatively high SC transition temperature is closely related to doped CuO_2 planes. It has been argued that the essential physics of the doped CuO_2 plane is contained in the t-J model on a square lattice[1],

$$H=-t\sum_{i\hat{\eta}\sigma}C^{\dagger}_{i\sigma}C_{i+\hat{\eta}\sigma}+\mu\sum_{i\sigma}C^{\dagger}_{i\sigma}C_{i\sigma}+J\sum_{i\hat{\eta}}\mathbf{S}_i\cdot\mathbf{S}_{i+\hat{\eta}}, \tag{1}$$

with $\hat{\eta}=\pm\hat{x},\pm\hat{y}$, $C^{\dagger}_{i\sigma}$ ($C_{i\sigma}$) is the electron creation (annihilation) operator, $\mathbf{S}_i=C^{\dagger}_i\vec{\sigma}C_i/2$ is spin operator with $\vec{\sigma}=(\sigma_x,\sigma_y,\sigma_z)$ as Pauli matrices, and μ is the chemical potential. The t-J model (1) is subject to an important local constraint to avoid the double occupancy, i.e., $\sum_{\sigma}C^{\dagger}_{i\sigma}C_{i\sigma}\leq 1$. In the t-J model, the strong electron correlation manifests itself by this single occupancy local constraint, and therefore the crucial requirement is to impose this local constraint. This local constraint can be treated properly in analytical calculations within the CSS fermion-spin theory[18], where the constrained electron operators are decoupled as, $C_{i\uparrow}=h^{\dagger}_{i\uparrow}S^{-}_i$ and $C_{i\downarrow}=h^{\dagger}_{i\downarrow}S^{+}_i$, with the spinful fermion operator $h_{i\sigma}=e^{-i\Phi_{i\sigma}}h_i$ describes the charge degree of freedom together with some effects of the spin configuration rearrangements due to the presence of the hole itself (dressed holon), while the spin operator S_i describes the spin degree of freedom (dressed spin), then the electron local constraint for the single occupancy is satisfied in analytical calculations[18]. In this CSS fermion-spin representation, the low-energy behavior of the t-J model (1) can be expressed as[17–19],

$$\begin{aligned}H=&-t\sum_{i\hat{\eta}}(h_{i\uparrow}S^{+}_i h^{\dagger}_{i+\hat{\eta}\uparrow}S^{-}_{i+\hat{\eta}}+h_{i\downarrow}S^{-}_i h^{\dagger}_{i+\hat{\eta}\downarrow}S^{+}_{i+\hat{\eta}})\\&-\mu\sum_{i\sigma}h^{\dagger}_{i\sigma}h_{i\sigma}+J_{\rm eff}\sum_{i\hat{\eta}}\mathbf{S}_i\cdot\mathbf{S}_{i+\hat{\eta}},\end{aligned} \tag{2}$$

with $J_{\rm eff}=(1-x)^2J$, and $x=\langle h^{\dagger}_{i\sigma}h_{i\sigma}\rangle=\langle h^{\dagger}_i h_i\rangle$ is the hole doping concentration. As a consequence, the kinetic energy (t) term in the t-J model has been expressed as the dressed holon-spin interaction, which reflects that even kinetic energy term in the t-J model has strong Coulombic contributions due to the restriction of single occupancy of a given site. This dressed holon-spin interaction is quite strong, and we[17,19] have shown in terms of Eliashberg's strong coupling theory[20,21] that in the case without AFLRO, this interaction can induce the dressed holon pairing state (then the electron Cooper pairing state) by exchanging dressed spin excitations in the higher power of the hole doping concentration x. The angle resolved photoemission spectroscopy (ARPES) measurements[22] have shown that in the real space the gap function and pairing force have a range of one lattice spacing, this indicates that the order parameter for the electron Cooper pair can be expressed as,

$$\begin{aligned}\Delta&=\langle C^{\dagger}_{i\uparrow}C^{\dagger}_{i+\hat{\eta}\downarrow}-C^{\dagger}_{i\downarrow}C^{\dagger}_{i+\hat{\eta}\uparrow}\rangle\\&=\langle h_{i\uparrow}h_{i+\hat{\eta}\downarrow}S^{+}_i S^{-}_{i+\hat{\eta}}-h_{i\downarrow}h_{i+\hat{\eta}\uparrow}S^{-}_i S^{+}_{i+\hat{\eta}}\rangle\\&=-\langle S^{+}_i S^{-}_{i+\hat{\eta}}\rangle\Delta_h,\end{aligned} \tag{3}$$

with the dressed holon pairing order parameter,

$$\Delta_h=\langle h_{i+\hat{\eta}\downarrow}h_{i\uparrow}-h_{i+\hat{\eta}\uparrow}h_{i\downarrow}\rangle, \tag{4}$$

which shows that the SC order parameter is closely related to the dressed holon pairing amplitude, and is proportional to the number of doped holes, and not to the number of electrons. Following our previous discussions[17,19], the self-consistent equations that satisfied by the full dressed holon diagonal and off-diagonal Green's functions are obtained as,

$$\begin{aligned}g(k)=&\,g^{(0)}(k)+g^{(0)}(k)[\Sigma^{(h)}_1(k)g(k)\\&-\Sigma^{(h)}_2(-k)\Im^{\dagger}(k)],\end{aligned} \tag{5a}$$

$$\begin{aligned}\Im^{\dagger}(k)=&\,g^{(0)}(-k)[\Sigma^{(h)}_1(-k)\Im^{\dagger}(-k)\\&+\Sigma^{(h)}_2(-k)g(k)],\end{aligned} \tag{5b}$$

respectively, where the four-vector notation $k=(\mathbf{k},i\omega_n)$, and the dressed holon self-energies are obtained as,

$$\begin{aligned}\Sigma^{(h)}_1(k)=&(Zt)^2\frac{1}{N^2}\sum_{\mathbf{p},\mathbf{p}'}\gamma^2_{\mathbf{p}+\mathbf{p}'+\mathbf{k}}\frac{1}{\beta}\sum_{ip_m}g(p+k)\\&\times\frac{1}{\beta}\sum_{ip'_m}D^{(0)}(p')D^{(0)}(p'+p),\end{aligned} \tag{6a}$$

$$\begin{aligned}\Sigma^{(h)}_2(k)=&(Zt)^2\frac{1}{N^2}\sum_{\mathbf{p},\mathbf{p}'}\gamma^2_{\mathbf{p}+\mathbf{p}'+\mathbf{k}}\frac{1}{\beta}\sum_{ip_m}\Im(-p-k)\\&\times\frac{1}{\beta}\sum_{ip'_m}D^{(0)}(p')D^{(0)}(p'+p),\end{aligned} \tag{6b}$$

where $p=(\mathbf{p},ip_m)$, $p'=(\mathbf{p}',ip'_m)$, and the dressed holon and spin mean-field (MF) Green's functions are evaluated as[17–19],

$$g^{(0)}(k)=\frac{1}{i\omega_n-\xi_{\mathbf{k}}}, \tag{7a}$$

$$D^{(0)}(p)=\frac{B_{\mathbf{p}}}{(ip_m)^2-\omega^2_{\mathbf{p}}}, \tag{7b}$$

with $B_{\mathbf{p}}=\lambda[2\chi_z(\epsilon\gamma_{\mathbf{p}}-1)+\chi(\gamma_{\mathbf{p}}-\epsilon)]$, $\lambda=2ZJ_{\rm eff}$, $\epsilon=1+2t\phi/J_{\rm eff}$, $\gamma_{\mathbf{p}}=(1/Z)\sum_{\hat{\eta}}e^{i\mathbf{p}\cdot\hat{\eta}}$, Z is the number of the nearest neighbor sites, the dressed spin correlation functions $\chi=\langle S^+_iS^-_{i+\hat{\eta}}\rangle$ and $\chi_z=\langle S^z_iS^z_{i+\hat{\eta}}\rangle$, and the MF dressed holon and spin excitation spectra are given by,

$$\xi_{\mathbf{k}}=Zt\chi\gamma_{\mathbf{k}}-\mu, \tag{8a}$$

$$\omega^2_{\mathbf{p}}=\lambda^2[(A_1-\alpha\epsilon\chi_z\gamma_{\mathbf{p}}-\frac{1}{2Z}\alpha\epsilon\chi)(1-\epsilon\gamma_{\mathbf{p}}) +\frac{1}{2}\epsilon(A_2-\frac{1}{2}\alpha\chi_z-\alpha\chi\gamma_{\mathbf{p}})(\epsilon-\gamma_{\mathbf{p}})], \tag{8b}$$

where $A_1=\alpha C^z+(1-\alpha)/(4Z)$, $A_2=\alpha C+(1-\alpha)/(2Z)$, the dressed holon particle-hole parameter $\phi=\langle h^\dagger_{i\sigma}h_{i+\hat{\eta}\sigma}\rangle$, and the dressed spin correlation functions $C=(1/Z^2)\sum_{\hat{\eta},\hat{\eta}'}\langle S^+_{i+\hat{\eta}}S^-_{i+\hat{\eta}'}\rangle$ and $C_z=(1/Z^2)\sum_{\hat{\eta},\hat{\eta}'}\langle S^z_{i+\hat{\eta}}S^z_{i+\hat{\eta}'}\rangle$. In order to satisfy the sum rule of the dressed spin correlation function $\langle S^+_iS^-_i\rangle=1/2$ in the case without AFLRO, the important decoupling parameter α has been introduced in the MF calculation[23,24]. In the calculation of the self-energies (6), the dressed spin part has been limited to the MF level[17], i.e., the full dressed spin Green's function in Eq. (6) has been replaced by the MF dressed spin Green's function (7b), since the normal-state charge transport obtained at this level can well describe the experimental data[18,25].

Since the pairing force and dressed holon gap function have been incorporated into the self-energy function $\Sigma^{(h)}_2(k)$, then it is called as the effective dressed holon gap function. On the other hand, the self-energy function $\Sigma^{(h)}_1(k)$ renormalizes the MF dressed holon spectrum, and therefore it describes the quasiparticle coherence. Moreover, $\Sigma^{(h)}_2(k)$ is an even function of $i\omega_n$, while $\Sigma^{(h)}_1(k)$ is not. In this case, it is convenient to break $\Sigma^{(h)}_1(k)$ up into its symmetric and antisymmetric parts as, $\Sigma^{(h)}_1(k)=\Sigma^{(h)}_{1e}(k)+i\omega_n\Sigma^{(h)}_{1o}(k)$, where $\Sigma^{(h)}_{1e}(k)$ and $\Sigma^{(h)}_{1o}(k)$ are both even functions of $i\omega_n$. Now we define the charge carrier quasiparticle coherent weight $Z^{-1}_F(k)=1-\Sigma^{(h)}_{1o}(k)$, then the dressed holon diagonal and off-diagonal Green's functions in Eq. (5) can be expressed as,

$$g(k)=\frac{i\omega_n/Z_F(k)+\xi_{\mathbf{k}}+\Sigma^{(h)}_{1e}(k)}{[i\omega_n/Z_F(k)]^2-[\xi_{\mathbf{k}}+\Sigma^{(h)}_{1e}(k)]^2-[\Sigma^{(h)}_2(k)]^2}, \tag{9a}$$

$$\Im^\dagger(k)=\frac{-\Sigma^{(h)}_2(k)}{[i\omega_n/Z_F(k)]^2-[\xi_{\mathbf{k}}+\Sigma^{(h)}_{1e}(k)]^2-[\Sigma^{(h)}_2(k)]^2}. \tag{9b}$$

As in the conventional superconductor[20], the retarded function ${\rm Re}\Sigma^{(h)}_{1e}(k)$ may be a constant, independent of $(\mathbf{k},\omega)$. It just renormalizes the chemical potential, and therefore can be neglected. Furthermore, we only study the static limit of the effective dressed holon gap function and quasiparticle coherent weight, i.e., $\Sigma^{(h)}_2(k)=\bar{\Delta}_h(\mathbf{k})$, and $Z^{-1}_F(\mathbf{k})=1-\Sigma^{(h)}_{1o}(\mathbf{k})$. In this case, the dressed holon diagonal and off-diagonal Green's functions in Eq. (9) can be rewritten explicitly as,

$$g(k)=\frac{1}{2}\left(1+\frac{\bar{\xi_{\mathbf{k}}}}{E_{\mathbf{k}}}\right)\frac{Z_F(\mathbf{k})}{i\omega_n-E_{\mathbf{k}}} +\frac{1}{2}\left(1-\frac{\bar{\xi_{\mathbf{k}}}}{E_{\mathbf{k}}}\right)\frac{Z_F(\mathbf{k})}{i\omega_n+E_{\mathbf{k}}}, \tag{10a}$$

$$\Im^\dagger(k)=-\frac{1}{2}\frac{\bar{\Delta}_{hZ}(\mathbf{k})}{E_{\mathbf{k}}}Z_F(\mathbf{k})\left(\frac{1}{i\omega_n-E_{\mathbf{k}}} -\frac{1}{i\omega_n+E_{\mathbf{k}}}\right), \tag{10b}$$

with $\bar{\xi_{\mathbf{k}}}=Z_F(\mathbf{k})\xi_{\mathbf{k}}$, $\bar{\Delta}_{hZ}(\mathbf{k})=Z_F(\mathbf{k})\bar{\Delta}_h(\mathbf{k})$, and the dressed holon quasiparticle spectrum $E_{\mathbf{k}}=\sqrt{\bar{\xi}^2_{\mathbf{k}}+\mid\bar{\Delta}_{hZ}(\mathbf{k})\mid^2}$, this $Z_F(\mathbf{k})$ reduces the dressed holon quasiparticle bandwidth. Although $Z_F(\mathbf{k})$ is still a function of $\mathbf{k}$, the wave vector dependence is unimportant, since everything happens at the electron Fermi surface (EFS). In this case, we will approximate $Z_F(\mathbf{k})$ by a constant, $Z_F=Z_F(\mathbf{k}_0)$, where the special wave vector $\mathbf{k}_0$ is defined below. In the CSS fermion-spin theory, the electron diagonal Green's function $G(i-j,t-t')=\langle\langle C_{i\sigma}(t);C^\dagger_{j\sigma}(t')\rangle\rangle$ is a convolution of the dressed spin Green's function and dressed holon diagonal Green's function, which reflects the charge-spin recombination[2], and in the present case, it can be calculated in terms of Eqs. (7b) and (10a) as[23],

$$\begin{aligned}G(k)&=\frac{1}{N}\sum_{\mathbf{p}}\int^\infty_{-\infty}\frac{d\omega'}{2\pi}\frac{d\omega''}{2\pi}A_s(\mathbf{p},\omega')A_h(\mathbf{p}-\mathbf{k},\omega'')\\ &\times\frac{n_F(\omega'')+n_B(\omega')}{i\omega_n+\omega''-\omega'}\\ &=\frac{1}{N}\sum_{\mathbf{p}}Z_F(\mathbf{p}-\mathbf{k})\frac{B_{\mathbf{p}}}{4\omega_{\mathbf{p}}}\left\{\left(1+\frac{\bar{\xi}_{\mathbf{p}-\mathbf{k}}}{E_{\mathbf{p}-\mathbf{k}}}\right)\right.\\ &\times\left(\frac{L_1(\mathbf{k},\mathbf{p})}{i\omega_n+E_{\mathbf{p}-\mathbf{k}}-\omega_{\mathbf{p}}}+\frac{L_2(\mathbf{k},\mathbf{p})}{i\omega_n+E_{\mathbf{p}-\mathbf{k}}+\omega_{\mathbf{p}}}\right)\\ &+\left(1-\frac{\bar{\xi}_{\mathbf{p}-\mathbf{k}}}{E_{\mathbf{p}-\mathbf{k}}}\right)\left(\frac{L_2(\mathbf{k},\mathbf{p})}{i\omega_n-E_{\mathbf{p}-\mathbf{k}}-\omega_{\mathbf{p}}}\right.\\ &\left.\left.+\frac{L_1(\mathbf{k},\mathbf{p})}{i\omega_n-E_{\mathbf{p}-\mathbf{k}}+\omega_{\mathbf{p}}}\right)\right\},\end{aligned} \tag{11}$$

where the MF dressed spin spectral function $A_s(\mathbf{k},\omega)=-2{\rm Im}D^{(0)}(\mathbf{k},\omega)$, the dressed holon spectral function $A_h(\mathbf{k},\omega)=-2{\rm Im}g(\mathbf{k},\omega)$, $L_1(\mathbf{k},\mathbf{p})=n_F(E_{\mathbf{p}-\mathbf{k}})+n_B(\omega_{\mathbf{p}})$, $L_2(\mathbf{k},\mathbf{p})=1-n_F(E_{\mathbf{p}-\mathbf{k}})+n_B(\omega_{\mathbf{p}})$, and $n_B(\omega)$ and $n_F(\omega)$ are the boson and fermion distribution functions, respectively. Then the electron quasiparticle dispersion is determined by the poles of the electron diagonal Green's function (11). At the half-filling, the t-J

model is reduced to the AF Heisenberg model, where there is no charge degree of freedom, and then the dressed holon excitation spectrum disappears, while the electron quasiparticle dispersion is reduced as the spin excitation spectrum[26]. This electron diagonal Green's function can be used to extract the electron momentum distribution (then EFS) as[23],

$$n_{\mathbf{k}} = \frac{1}{2} - \frac{1}{N}\sum_{\mathbf{p}} n_s(\mathbf{p}) \int_{-\infty}^{\infty} \frac{d\omega}{2\pi} A_h(\mathbf{p}-\mathbf{k},\omega) n_F(\omega), \quad (12)$$

with $n_s(\mathbf{p}) = \int_{-\infty}^{\infty} d\omega A_s(\mathbf{p},\omega) n_s(\omega)/2\pi$ is the dressed spin momentum distribution. Then this electron momentum distribution can be evaluated explicitly in terms of the MF dressed spin Green's function (7b) and dressed holon diagonal Green's function (10a) as,

$$n_{\mathbf{k}} = \frac{1}{2} - \frac{1}{2N}\sum_{\mathbf{p}} n_s^{(0)}(\mathbf{p}) Z_F(\mathbf{p}-\mathbf{k}) \times \left(1 - \frac{\bar{\xi}_{\mathbf{p}-\mathbf{k}}}{E_{\mathbf{p}-\mathbf{k}}} \tanh[\frac{1}{2}\beta E_{\mathbf{p}-\mathbf{k}}]\right), \quad (13)$$

with $n_s^{(0)}(\mathbf{p}) = B_{\mathbf{p}} \coth(\beta\omega_{\mathbf{p}}/2)/(2\omega_{\mathbf{p}})$. Since the dressed spins center around $[\pm\pi,\pm\pi]$ in the Brillouin zone at the MF level[23], then the electron momentum distribution (13) can be approximately reduced as,

$$n_{\mathbf{k}} \approx 1/2 - \rho_s^{(0)} Z_F(\mathbf{k_A}-\mathbf{k}) \times [1 - \bar{\xi}_{\mathbf{k_A}-\mathbf{k}} \tanh(\beta E_{\mathbf{k_A}-\mathbf{k}}/2)/E_{\mathbf{k_A}-\mathbf{k}}]/2, \quad (14)$$

with $\mathbf{k_A} = [\pi,\pi]$, and $\rho_s^{(0)} = (1/N)\sum_{\mathbf{p}=(\pm\pi,\pm\pi)} n_s^{(0)}(\mathbf{p})$. It has been shown from ARPES experiments[27] that EFS is small pockets around $[\pi/2,\pi/2]$ at small doping, and becomes a large EFS at large doping. Therefore in the present case the Fermi wave vector from above electron momentum distribution can be estimated qualitatively[23] as $\mathbf{k_F} \approx [(1-x)\pi/2,(1-x)\pi/2]$, and is evolution with doping. Then the wave vector $\mathbf{k}_0$ is obtained as $\mathbf{k}_0 = \mathbf{k_A} - \mathbf{k_F}$, and we only need to calculate $Z_F = Z_F(\mathbf{k}_0)$ as mentioned above. Since the charge-spin recombination from the convolution of the dressed spin Green's function and dressed holon diagonal Green's function leads to form EFS[2], then the dressed holon quasiparticle coherence Z_F appearing in the electron momentum distribution also reflects the electron quasiparticle coherence. We emphasize that the Fermi wave vector $\mathbf{k_F}$ estimated in the present case only is qualitative correct, while the quantitative correct EFS obtained within the t-J model is an rather complicated problem, and one may need to consider the vertex corrections. This and related theoretical ARPES results are under investigations now.

Some experiments seem consistent with an s-wave pairing[28], while other measurements gave the evidence in favor of the d-wave pairing[29,30]. This reflects a fact that the d-wave gap function $\propto \mathrm{k}_x^2 - \mathrm{k}_y^2$ belongs to the same representation Γ_1 of the orthorhombic crystal group as does s-wave gap function $\propto \mathrm{k}_x^2 + \mathrm{k}_y^2$. Within some strong correlated models, the earlier numerical simulations[31] have shown that the s-wave channel was competitive with the d-wave, which indicates that superconductivity with both s-wave and d-wave symmetries may arise directly from the repulsive interactions. For understanding of these experimental results, we consider both s-wave and d-wave cases, i.e., $\bar{\Delta}_{hZ}^{(s)}(\mathbf{k}) = \bar{\Delta}_{hZ}^{(s)}\gamma_{\mathbf{k}}^{(s)}$, with $\gamma_{\mathbf{k}}^{(s)} = \gamma_{\mathbf{k}} = (\cos k_x + \cos k_y)/2$, for the s-wave pairing, and $\bar{\Delta}_{hZ}^{(d)}(\mathbf{k}) = \bar{\Delta}_{hZ}^{(d)}\gamma_{\mathbf{k}}^{(d)}$, with $\gamma_{\mathbf{k}}^{(d)} = (\cos k_x - \cos k_y)/2$, for the d-wave pairing, respectively. In this case, the dressed holon effective gap parameter and quasiparticle coherent weight in Eq. (6) satisfy the following two equations[17,19],

$$1 = (Zt)^2 \frac{1}{N^3}\sum_{\mathbf{k},\mathbf{q},\mathbf{p}} \gamma_{\mathbf{k}+\mathbf{q}}^2 \gamma_{\mathbf{k}-\mathbf{p}+\mathbf{q}}^{(a)} \gamma_{\mathbf{k}}^{(a)} \frac{Z_F^2}{E_{\mathbf{k}}} \frac{B_{\mathbf{q}} B_{\mathbf{p}}}{\omega_{\mathbf{q}}\omega_{\mathbf{p}}} \times \left(\frac{F_1^{(1)}(\mathbf{k},\mathbf{q},\mathbf{p})}{(\omega_{\mathbf{p}}-\omega_{\mathbf{q}})^2 - E_{\mathbf{k}}^2} + \frac{F_1^{(2)}(\mathbf{k},\mathbf{q},\mathbf{p})}{(\omega_{\mathbf{p}}+\omega_{\mathbf{q}})^2 - E_{\mathbf{k}}^2}\right), \quad (15a)$$

$$Z_F^{-1} = 1 + (Zt)^2 \frac{1}{N^2}\sum_{\mathbf{q},\mathbf{p}} \gamma_{\mathbf{p}+\mathbf{k}_0}^2 Z_F \frac{B_{\mathbf{q}} B_{\mathbf{p}}}{4\omega_{\mathbf{q}}\omega_{\mathbf{p}}} \times \left(\frac{F_2^{(1)}(\mathbf{q},\mathbf{p})}{(\omega_{\mathbf{p}}-\omega_{\mathbf{q}}-E_{\mathbf{p}-\mathbf{q}+\mathbf{k}_0})^2} + \frac{F_2^{(2)}(\mathbf{q},\mathbf{p})}{(\omega_{\mathbf{p}}-\omega_{\mathbf{q}}+E_{\mathbf{p}-\mathbf{q}+\mathbf{k}_0})^2} + \frac{F_2^{(3)}(\mathbf{q},\mathbf{p})}{(\omega_{\mathbf{p}}+\omega_{\mathbf{q}}-E_{\mathbf{p}-\mathbf{q}+\mathbf{k}_0})^2} + \frac{F_2^{(4)}(\mathbf{q},\mathbf{p})}{(\omega_{\mathbf{p}}+\omega_{\mathbf{q}}+E_{\mathbf{p}-\mathbf{q}+\mathbf{k}_0})^2}\right), \quad (15b)$$

respectively, where $a = \mathrm{s}, \mathrm{d}$, $F_1^{(1)}(\mathbf{k},\mathbf{q},\mathbf{p}) = (\omega_{\mathbf{p}}-\omega_{\mathbf{q}})[n_B(\omega_{\mathbf{q}}) - n_B(\omega_{\mathbf{p}})][1 - 2n_F(E_{\mathbf{k}})] + E_{\mathbf{k}}[n_B(\omega_{\mathbf{p}})n_B(-\omega_{\mathbf{q}}) + n_B(\omega_{\mathbf{q}})n_B(-\omega_{\mathbf{p}})]$, $F_1^{(2)}(\mathbf{k},\mathbf{q},\mathbf{p}) = -(\omega_{\mathbf{p}}+\omega_{\mathbf{q}})[n_B(\omega_{\mathbf{q}}) - n_B(-\omega_{\mathbf{p}})][1 - 2n_F(E_{\mathbf{k}})] + E_{\mathbf{k}}[n_B(\omega_{\mathbf{p}})n_B(\omega_{\mathbf{q}}) + n_B(-\omega_{\mathbf{p}})n_B(-\omega_{\mathbf{q}})]$, $F_2^{(1)}(\mathbf{q},\mathbf{p}) = n_F(E_{\mathbf{p}-\mathbf{q}+\mathbf{k}_0})[n_B(\omega_{\mathbf{q}}) - n_B(\omega_{\mathbf{p}})] - n_B(\omega_{\mathbf{p}})n_B(-\omega_{\mathbf{q}})$, $F_2^{(2)}(\mathbf{q},\mathbf{p}) = n_F(E_{\mathbf{p}-\mathbf{q}+\mathbf{k}_0})[n_B(\omega_{\mathbf{p}}) - n_B(\omega_{\mathbf{q}})] - n_B(\omega_{\mathbf{q}})n_B(-\omega_{\mathbf{p}})$, $F_2^{(3)}(\mathbf{q},\mathbf{p}) = n_F(E_{\mathbf{p}-\mathbf{q}+\mathbf{k}_0})[n_B(\omega_{\mathbf{q}}) - n_B(-\omega_{\mathbf{p}})] + n_B(\omega_{\mathbf{p}})n_B(\omega_{\mathbf{q}})$, and $F_2^{(4)}(\mathbf{q},\mathbf{p}) = n_F(E_{\mathbf{p}-\mathbf{q}+\mathbf{k}_0})[n_B(-\omega_{\mathbf{q}}) - n_B(\omega_{\mathbf{p}})] + n_B(-\omega_{\mathbf{p}})n_B(-\omega_{\mathbf{q}})$. These two equations are in control of the SC order directly, and must be solved simultaneously with other self-consistent equations as shown in Ref.[17], then all order parameters, decoupling parameter α, and chemical potential μ are determined by the self-consistent calculation[17]. In this case, we obtain the dressed holon pair gap function in terms of the off-diagonal Green's function (10b) as[20],

$$\Delta_h^{(a)}(\mathbf{k}) = -\frac{1}{\beta}\sum_{i\omega_n} \Im^{\dagger}(\mathbf{k}, i\omega_n)$$

$$= \frac{1}{2} Z_F \frac{\bar{\Delta}^{(a)}_{hZ}(\mathbf{k})}{E_{\mathbf{k}}} \tanh[\frac{1}{2}\beta E_{\mathbf{k}}], \quad (16)$$

then the dressed holon pair order parameter in Eq. (4) can be evaluated explicitly as,

$$\Delta^{(a)}_h = \frac{2}{N}\sum_{\mathbf{k}} [\gamma^{(a)}_{\mathbf{k}}]^2 \frac{Z_F \bar{\Delta}^{(a)}_{hZ}}{E_{\mathbf{k}}} \tanh[\frac{1}{2}\beta E_{\mathbf{k}}]. \quad (17)$$

We[17,19] have shown that this dressed holon pairing state originating from the kinetic energy term by exchanging dressed spin excitations can lead to form the electron Cooper pairing state, where the SC gap function is obtained from the electron off-diagonal Green's function $I^{\dagger}(i-j,t-t') = \langle\langle C^{\dagger}_{i\uparrow}(t); C^{\dagger}_{j\downarrow}(t')\rangle\rangle$, which is a convolution of the dressed spin Green's function and dressed holon off-diagonal Green's function[2], and in the present case can be obtained in terms of the dressed spin MF Green's function (7b) and dressed holon off-diagonal Green's function (10b) as,

$$I^{\dagger}(k) = \frac{1}{N}\sum_{\mathbf{p}} \frac{Z_F \bar{\Delta}^{(a)}_{hZ}(\mathbf{p}-\mathbf{k})}{E_{\mathbf{p}-\mathbf{k}}} \frac{B_{\mathbf{p}}}{2\omega_{\mathbf{p}}} \times \left(\frac{(\omega_{\mathbf{p}} + E_{\mathbf{p}-\mathbf{k}})[n_B(\omega_{\mathbf{p}}) + n_F(-E_{\mathbf{p}-\mathbf{k}})]}{(i\omega_n)^2 - (\omega_{\mathbf{p}} + E_{\mathbf{p}-\mathbf{k}})^2} - \frac{(\omega_{\mathbf{p}} - E_{\mathbf{p}-\mathbf{k}})[n_B(\omega_{\mathbf{p}}) + n_F(E_{\mathbf{p}-\mathbf{k}})]}{(i\omega_n)^2 - (\omega_{\mathbf{p}} - E_{\mathbf{p}-\mathbf{k}})^2} \right), \quad (18)$$

then the SC gap function is obtained from this electron off-diagonal Green's function as,

$$\Delta^{(a)}(\mathbf{k}) = -\frac{1}{\beta}\sum_{i\omega_n} I^{\dagger}(\mathbf{k}, i\omega_n) = -\frac{1}{N}\sum_{\mathbf{p}} \frac{Z_F \bar{\Delta}^{(a)}_{Zh}(\mathbf{p}-\mathbf{k})}{2E_{\mathbf{p}-\mathbf{k}}} \tanh[\frac{1}{2}\beta E_{\mathbf{p}-\mathbf{k}}] \times \frac{B_{\mathbf{p}}}{2\omega_{\mathbf{p}}} \coth[\frac{1}{2}\beta\omega_{\mathbf{p}}], \quad (19)$$

which shows that the symmetry of the electron Cooper pair is determined by the symmetry of the dressed holon pair[17], and therefore the SC gap function can be written as $\Delta^{(a)}(\mathbf{k}) = \Delta^{(a)}\gamma^{(a)}_{\mathbf{k}}$, then the SC gap parameter in Eq. (3) is evaluated in terms of Eqs. (19) and (17) as $\Delta^{(a)} = -\chi\Delta^{(a)}_h$. Since the dressed holon (then electron) pairing interaction also is doping dependent, then the experimental observed SC gap parameter should be the effective SC gap parameter $\bar{\Delta}^{(a)} \sim -\chi\bar{\Delta}^{(a)}_h$. In Fig. 1, we plot the effective dressed holon pairing (a) and effective SC (b) gap parameters in the s-wave symmetry (solid line) and d-wave symmetry (dashed line) as a function of the hole doping concentration x at $T = 0.002J$ and $t/J = 2.5$. For comparison, the experimental result[32] of the upper critical field as a function of the hole doping concentration is also shown in Fig. 1(b). In a given doping concentration, the upper critical field is defined as the critical field that destroys the SC-state at the zero temperature in the given doping concentration, therefore the upper critical field also measures the strength of the binding of electrons into Cooper pairs like the effective SC gap parameter[32]. In other words, both effective SC gap parameter and upper critical field have a similar doping dependence[32]. In this sense, our result is in qualitative agreement with the experimental data[32]. In particular, the value of $\bar{\Delta}^{(d)}$ increases with increasing doping in the underdoped regime, and reaches a maximum in the optimal doping $x_{\rm opt} \approx 0.18$, then decreases in the overdoped regime.

The present result in Eq. (19) also shows that the SC transition temperature $T^{(a)}_c$ occurring in the case of the SC gap parameter $\Delta^{(a)} = 0$ is identical to the dressed holon pair transition temperature occurring in the case of the effective dressed holon pairing gap parameter $\bar{\Delta}^{(a)}_h = 0$. In correspondence with the SC gap parameter, the SC transition temperature $T^{(a)}_c$ as a function of the hole doping concentration x in the s-wave (solid

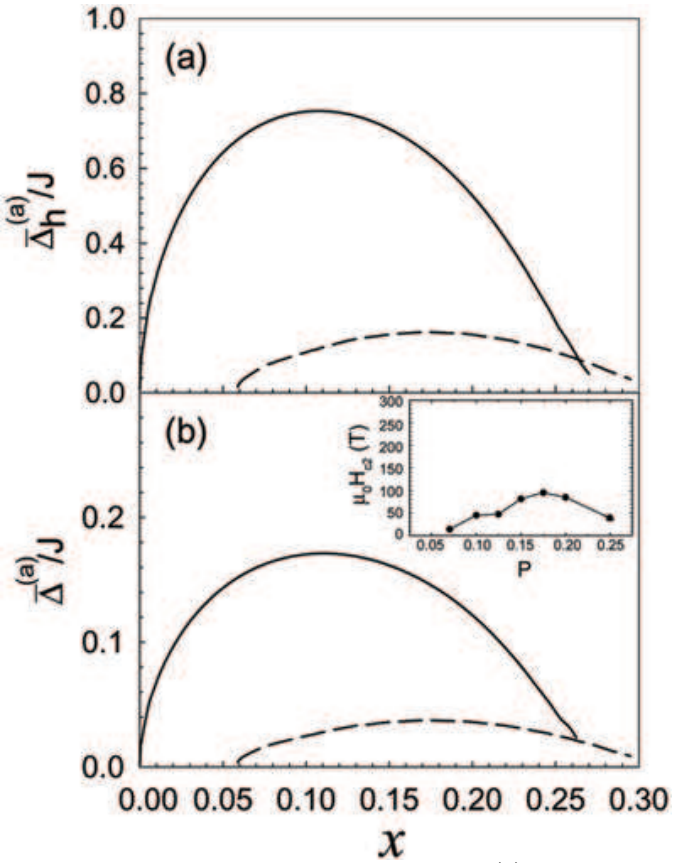

FIG. 1. The effective dressed holon pairing (a) and effective superconducting (b) gap parameters in the s-wave symmetry (solid line) and d-wave symmetry (dashed line) as a function of the hole doping concentration in $T = 0.002J$ and $t/J = 2.5$. Inset: the experimental result of the upper critical field as a function of the hole doping concentration taken from Ref. [32].

line) and d-wave (dashed line) symmetries for $t/J = 2.5$ is plotted in Fig. 2 in comparison with the experimental result[5] (inset). For the s-wave symmetry, the maximal SC transition temperature $T_c^{(s)}$ occurs around a particular doping concentration $x \approx 0.11$, and then decreases in both lower doped and higher doped regimes. However, for the d-wave symmetry, the maximal SC transition temperature $T_c^{(d)}$ occurs around the optimal doping concentration $x_{\rm opt} \approx 0.18$, and then decreases in both underdoped and overdoped regimes. Although the SC pairing symmetry is doping dependent, the SC state has the d-wave symmetry in a wide range of doping, in qualitative agreement with the experiments[33–35]. Furthermore, $T_c^{(d)}$ in the underdoped regime ($T_c^{(s)}$ in the lower doped regime) is proportional to the hole doping concentration x, and therefore $T_c^{(d)}$ in the underdoped regime

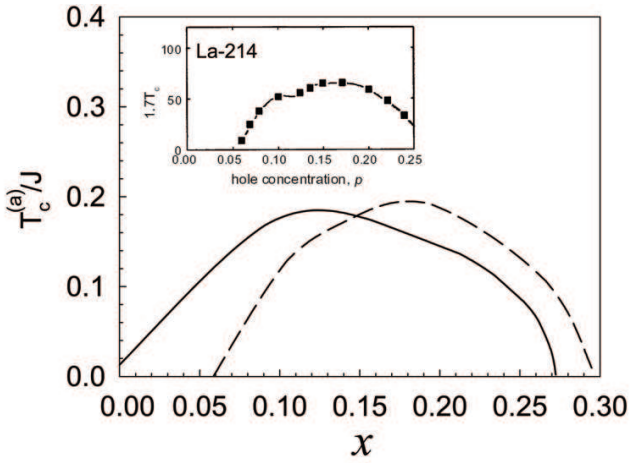

FIG. 2. The superconducting transition temperature as a function of the hole doping concentration in the s-wave symmetry (solid line) and d-wave symmetry (dashed line) for $t/J = 2.5$. Inset: the experimental result taken from Ref. [5].

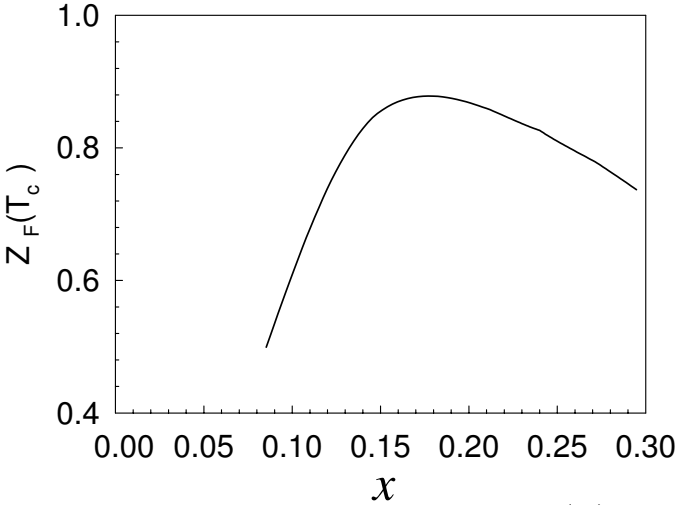

FIG. 3. The quasiparticle coherent weight $Z_F(T_c)$ as a function of the hole doping concentration for $t/J = 2.5$.

($T_c^{(s)}$ in the lower doped regime) is set by the hole doping concentration[36], this reflects that the density of the dressed holons directly determines the superfluid density in the underdoped regime for the d-wave case (the lower doped regime for the s-wave case). Using an reasonably estimative value of $J \sim 800$K to 1200K in doped cuprates, the SC transition temperature in the optimal doping is $T_c^{(d)} \approx 0.2J \approx 160\text{K} \sim 240\text{K}$, also in qualitative agreement with the experimental data[5,36,35].

In the present framework of the kinetic energy driven superconductivity, the antisymmetric part of the self-energy function $\Sigma_{1o}^{(h)}(\mathbf{k})$ (then Z_F) describes the quasiparticle coherence, and therefore Z_F is closely related to the quasiparticle density, while the self-energy function $\Sigma_2^{(h)}(\mathbf{k})$ describes the effective dressed holon pairing gap function. Since the SC-order is established through an emerging quasiparticle[6], therefore the SC-order is controlled by both gap function and quasiparticle coherence, and is reflected explicitly in the self-consistent equations (15a) and (15b). To show this point clearly, we plot the quasiparticle coherent weight $Z_F(T_c)$ as a function of the hole doping concentration x for $t/J = 2.5$ in Fig. 3. As seen from Fig. 3, the doping dependent behavior of the quasiparticle coherent weight resembles that of the superfluid density in doped cuprates, i.e., Z_F grows linearly with the hole doping concentration in the underdoped and optimally doped regimes, and then decreases with increasing doping in the overdoped regime, which leads to that the SC transition temperature reaches a maximum in the optimal doping, and then decreases in both underdoped and overdoped regimes. In comparison with Ref.[17], we therefore find that the quasiparticle coherence plays an important role in the kinetic energy driven superconductivity of doped cuprates. Since cuprate superconductors are highly anisotropic materials, therefore the effective SC gap function $\bar{\Delta}^{(s)}(\mathbf{k}) = \bar{\Delta}^{(s)}(\cos k_x + \cos k_y)/2$ for the s-wave symmetry or $\bar{\Delta}^{(d)}(\mathbf{k}) = \bar{\Delta}^{(d)}(\cos k_x - \cos k_y)/2$ for the d-wave case is dependent on the momentum. According to a comparison of the density of states as measured by scanning tunnelling microscopy[37] and ARPES spectral function[6] at $[\pi, 0]$ point on identical samples, it has been shown that the most contributions of the electronic states come from $[\pi, 0]$ point. In this case, although the value of the effective SC gap parameter $\bar{\Delta}^{(s)}$ (then the ratio $\bar{\Delta}^{(s)}/T_c^{(s)}$) for the s-wave symmetry is larger than these $\bar{\Delta}^{(d)}$ (then the ratio $\bar{\Delta}^{(d)}/T_c^{(d)}$) in the d-wave case, the system has the SC transition temperature $T_c^{(d)}$ with the d-wave symmetry in a wide range of doping.

III. DOPING AND ENERGY DEPENDENT MAGNETIC EXCITATIONS

In the CSS fermion-spin theory, the AF fluctuation is dominated by the scattering of the dressed spins[18,38].

Since in the normal-state the dressed spins move in the dressed holon background, therefore the dressed spin self-energy (then full dressed spin Green's function) in the normal-state has been obtained in terms of the collective mode in the dressed holon particle-hole channel[18,38]. With the help of this full dressed spin Green's function in the normal-state, the IC magnetic scattering and integrated spin response of doped cuprates in the normal-state have been discussed[18,38], and the results of the doping dependence of the incommensurability and integrated dynamical spin susceptibility are consistent with experimental results in the normal-state[4,8]. However, in the present SC-state discussed in Sec. II, the AF fluctuation has been incorporated into the electron off-diagonal Green's function (18) (hence the electron Cooper pair) in terms of the dressed spin Green's function, therefore there is a coexistence of the electron Cooper pair and AFSRC, and then AFSRC can persist into superconductivity[17]. Moreover, in the SC-state, the dressed spins move in the dressed holon pair background. In this case, we calculate the dressed spin self-energy (then the full dressed spin Green's function) in the SC-state in terms of the collective mode in the dressed holon particle-particle channel, and then give a theoretical explanation of the IC magnetic scattering peaks at both low and high energies and commensurate resonance peak at intermediate energy in the SC-state[7,8,10–15].

Following our previous discussions for the normal-state case[18,38], the full dressed spin Green's functions is expressed as,

$$D(\mathbf{k},\omega)=\frac{1}{D^{(0)-1}(\mathbf{k},\omega)-\Sigma^{(s)}(\mathbf{k},\omega)}, \tag{20}$$

with the second order spin self-energy $\Sigma^{(s)}(\mathbf{k},\omega)$. Within the framework of the equation of motion method[18,38], this self-energy in the SC-state with the d-wave symmetry is obtained from the dressed holon bubble in the dressed holon particle-particle channel as,

$$\Sigma^{(s)}(k)=(Zt)^2\frac{1}{N^2}\sum_{\mathbf{p},\mathbf{p}'}(\gamma^2_{\mathbf{p}'+\mathbf{p}+\mathbf{k}}+\gamma^2_{\mathbf{p}-\mathbf{k}}) \times\frac{1}{\beta}\sum_{ip'_m}D^{(0)}(p'+k)\frac{1}{\beta}\sum_{ip_m}\Im^{\dagger}(p)\Im(p+p'), \tag{21}$$

and can be evaluated explicitly in terms of the dressed holon off-diagonal Green's function (10b) and dressed spin MF Green's function (7b) as,

$$\Sigma^{(s)}(\mathbf{k},\omega)=(Zt)^2\frac{1}{N^2}\sum_{\mathbf{p},\mathbf{q}}(\gamma^2_{\mathbf{q}+\mathbf{p}+\mathbf{k}}+\gamma^2_{\mathbf{p}-\mathbf{k}}) \times\frac{B_{\mathbf{q}+\mathbf{k}}}{\omega_{\mathbf{q}+\mathbf{k}}}\frac{Z_F^2}{4}\frac{\bar{\Delta}^{(d)}_{hZ}(\mathbf{p})\bar{\Delta}^{(d)}_{hZ}(\mathbf{p}+\mathbf{q})}{E_{\mathbf{p}}E_{\mathbf{p}+\mathbf{q}}} \times\left(\frac{F_s^{(1)}(\mathbf{k},\mathbf{p},\mathbf{q})}{\omega^2-(E_{\mathbf{p}}-E_{\mathbf{p}+\mathbf{q}}+\omega_{\mathbf{q}+\mathbf{k}})^2} +\frac{F_s^{(2)}(\mathbf{k},\mathbf{p},\mathbf{q})}{\omega^2-(E_{\mathbf{p}+\mathbf{q}}-E_{\mathbf{p}}+\omega_{\mathbf{q}+\mathbf{k}})^2} +\frac{F_s^{(3)}(\mathbf{k},\mathbf{p},\mathbf{q})}{\omega^2-(E_{\mathbf{p}}+E_{\mathbf{p}+\mathbf{q}}+\omega_{\mathbf{q}+\mathbf{k}})^2} +\frac{F_s^{(4)}(\mathbf{k},\mathbf{p},\mathbf{q})}{\omega^2-(E_{\mathbf{p}+\mathbf{q}}+E_{\mathbf{p}}-\omega_{\mathbf{q}+\mathbf{k}})^2}\right), \tag{22}$$

where $F_s^{(1)}(\mathbf{k},\mathbf{p},\mathbf{q})=(E_{\mathbf{p}}-E_{\mathbf{p}+\mathbf{q}}+\omega_{\mathbf{q}+\mathbf{k}})\{n_B(\omega_{\mathbf{q}+\mathbf{k}})[n_F(E_{\mathbf{p}})-n_F(E_{\mathbf{p}+\mathbf{q}})]-n_F(E_{\mathbf{p}+\mathbf{q}})n_F(-E_{\mathbf{p}})\}$, $F_s^{(2)}(\mathbf{k},\mathbf{p},\mathbf{q})=(E_{\mathbf{p}+\mathbf{q}}-E_{\mathbf{p}}+\omega_{\mathbf{q}+\mathbf{k}})\{n_B(\omega_{\mathbf{q}+\mathbf{k}})[n_F(E_{\mathbf{p}+\mathbf{q}})-n_F(E_{\mathbf{p}})]-n_F(E_{\mathbf{p}})n_F(-E_{\mathbf{p}+\mathbf{q}})\}$, $F_s^{(3)}(\mathbf{k},\mathbf{p},\mathbf{q})=(E_{\mathbf{p}}+E_{\mathbf{p}+\mathbf{q}}+\omega_{\mathbf{q}+\mathbf{k}})\{n_B(\omega_{\mathbf{q}+\mathbf{k}})[n_F(-E_{\mathbf{p}})-n_F(E_{\mathbf{p}+\mathbf{q}})]+n_F(-E_{\mathbf{p}+\mathbf{q}})n_F(-E_{\mathbf{p}})\}$, $F_s^{(4)}(\mathbf{k},\mathbf{p},\mathbf{q})=(E_{\mathbf{p}}+E_{\mathbf{p}+\mathbf{q}}-\omega_{\mathbf{q}+\mathbf{k}})\{n_B(\omega_{\mathbf{q}+\mathbf{k}})[n_F(-E_{\mathbf{p}})-n_F(E_{\mathbf{p}+\mathbf{q}})]-n_F(E_{\mathbf{p}+\mathbf{q}})n_F(E_{\mathbf{p}})\}$. With the help of this full dressed spin Green's function, we can obtain the dynamical spin structure factor in the SC-state with the d-wave symmetry as,

$$S(\mathbf{k},\omega)=-2[1+n_B(\omega)]\mathrm{Im}D(\mathbf{k},\omega)=2[1+n_B(\omega)] \times\frac{B^2_{\mathbf{k}}\mathrm{Im}\Sigma^{(s)}(\mathbf{k},\omega)}{[\omega^2-\omega^2_{\mathbf{k}}-B_{\mathbf{k}}\mathrm{Re}\Sigma^{(s)}(\mathbf{k},\omega)]^2+[B_{\mathbf{k}}\mathrm{Im}\Sigma^{(s)}(\mathbf{k},\omega)]^2}, \tag{23}$$

where $\mathrm{Im}\Sigma^{(s)}(\mathbf{k},\omega)$ and $\mathrm{Re}\Sigma^{(s)}(\mathbf{k},\omega)$ are the imaginary and real parts of the second order spin self-energy in Eq. (18), respectively.

We are now ready to discuss the doping and energy dependent magnetic excitations in the SC-state. In Fig. 4, we plot the dynamical spin structure factor $S(\mathbf{k},\omega)$ in the (k_x,k_y) plane at the optimal doping $x_{\rm opt}=0.18$ with temperature $T=0.002J$ for parameter $t/J=2.5$ at energy (a) $\omega=0.13J$, (b) $\omega=0.35J$, and (c) $\omega=0.65J$, where the distinct feature is the presence of the IC-commensurate-IC transition in the spin fluctuation geometry. At low energy, the IC peaks are located at $[(1\pm\delta)/2,1/2]$ and $[1/2,(1\pm\delta)/2]$ (hereafter we use the units of $[2\pi,2\pi]$). However, these IC peaks are energy dependent, i.e., although these magnetic scattering peaks retain the IC pattern at $[(1\pm\delta)/2,1/2]$ and $[1/2,(1\pm\delta)/2]$ at low energy, the positions of the IC peaks move towards $[1/2,1/2]$ with increasing energy, and then the commensurate $[1/2,1/2]$ resonance peak appears at intermediate energy $\omega_r=0.35J$. This anticipated resonance energy $\omega_r=0.35J\approx 35$ mev (Ref.[39]) is not too far from the resonance energy ≈ 41 mev observed in optimally doped $YBa_2Cu_3O_{6+y}$[7,10–12]. Furthermore, the IC peaks are separated again above the resonance energy, and all IC peaks lie on a circle of radius of δ'. The values of δ' at high energy are different from the corresponding values of δ at low energy. Although some IC satellite parallel peaks appear, the main weight of the IC peaks is in the diagonal direction. Moreover, the separation at high energy gradually increases with increasing energy although the peaks have a weaker intensity than those

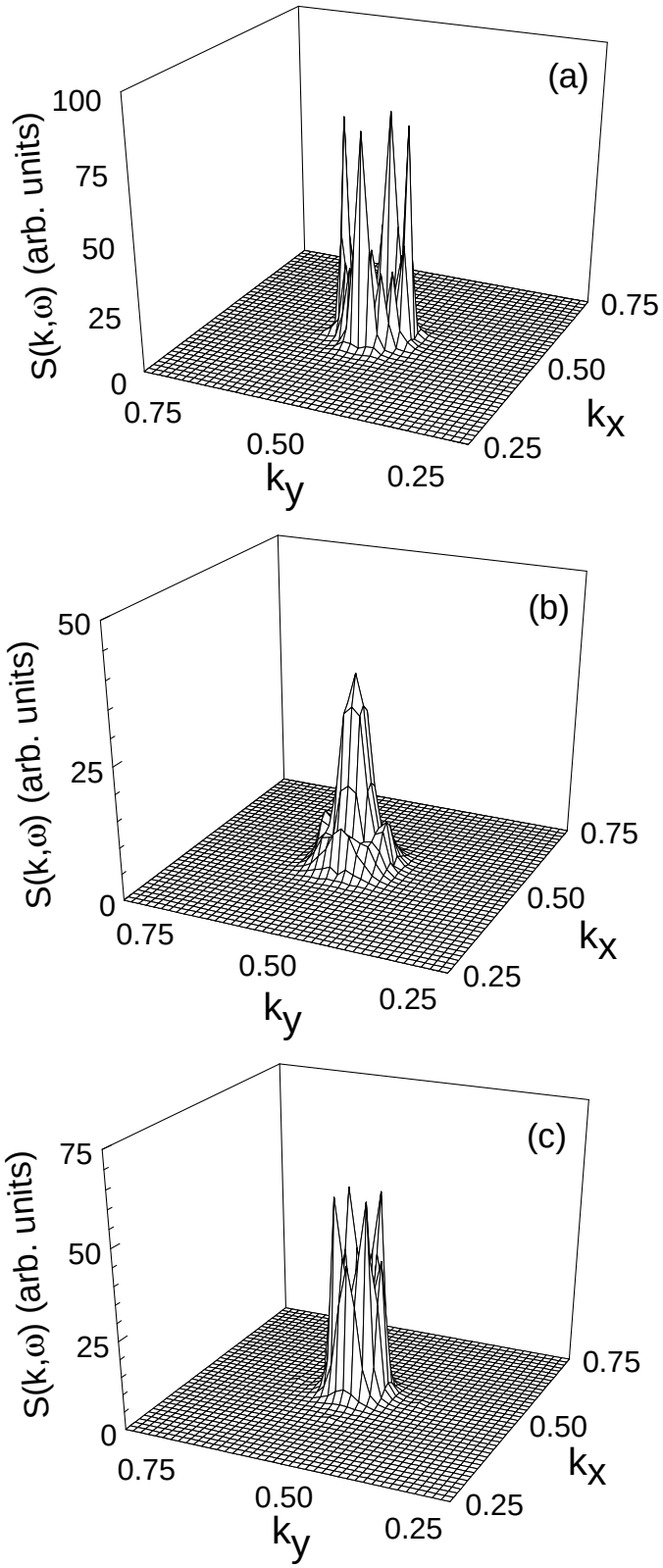

FIG. 4. The dynamical spin structure factor $S(\mathbf{k},\omega)$ in the (k_x, k_y) plane at $x_{\rm opt} = 0.18$ with $T = 0.002J$ for $t/J = 2.5$ at (a) $\omega = 0.13J$, (b) $\omega = 0.35J$, and (c) $\omega = 0.65J$.

below the resonance energy. To show this point clearly, we plot the evolution of the magnetic scattering peaks with energy at $x_{\rm opt} = 0.18$ in Fig. 5. For comparison, the experimental result[12] of $YBa_2Cu_3O_{6+y}$ with $y = 0.7$ ($x \approx 0.12$) in the SC-state is shown in the same figure. The similar experimental results[11,13] have also been obtained for $YBa_2Cu_3O_{6+y}$ with different doping concentrations. Our results show that there is a narrow energy range for the resonance peak, and therefore the dispersion at high energy is distinctly separated from the low energy IC fluctuations. The similar narrow energy range for the resonance peak has been observed from experiments[11]. The present results also show that in contrast to the case

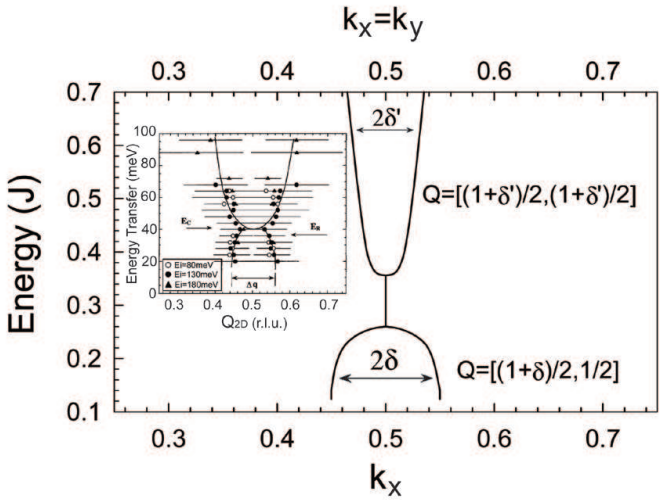

FIG. 5. The energy dependence of the position of the magnetic scattering peaks at $x_{\rm opt} = 0.18$ and $T = 0.002J$ for $t/J = 2.5$. Inset: the experimental result on $YBa_2Cu_3O_{6.85}$ in the superconducting-state taken from Ref. [12]

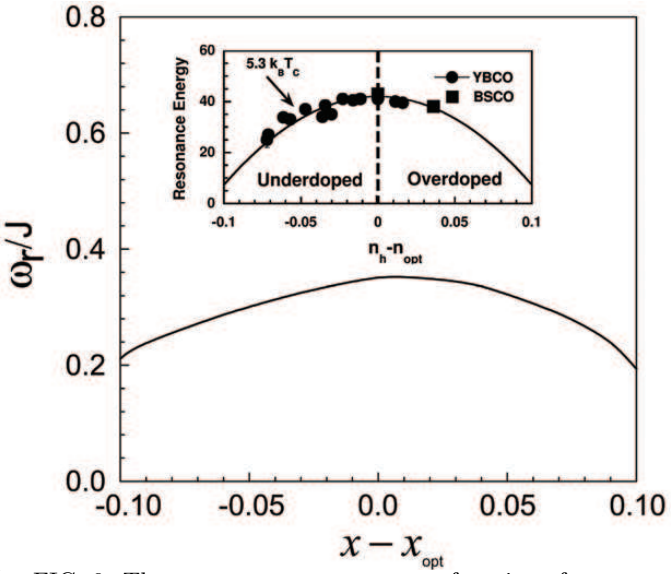

FIG. 6. The resonance energy ω_r as a function of $x - x_{\rm opt}$ in $T = 0.002J$ for $t/J = 2.5$. Inset: the experimental result taken from Ref. [10].

at low energy, the magnetic excitations at high energy disperse almost linearly with energy. Furthermore, the resonance energy ω_r as a function of doping $x - x_{\rm opt}$ in $T = 0.002J$ for $t/J = 2.5$ is plotted in Fig. 6 in comparison with the experimental result[10] (inset). It is shown that in analogy to the doping dependence of the SC transition temperature, the magnetic resonance energy ω_r increases with increasing doping in the underdoped regime, and reaches a maximum in the optimal doping, then decreases in the overdoped regime. These mediating dressed spin excitations in the SC-state are coupled to the conducting dressed holons (then electrons) under the kinetic energy driven SC mechanism[17], and have energy greater than the dressed holon pairing energy (then Cooper pairing energy). We have also made a series of scans for $S(\mathbf{k},\omega)$ at different temperatures, and found that those unusual magnetic excitations are present near the SC transition temperature. Although the simple t-J model can not be regarded as a comprehensive model for the quantitative comparison with cuprate superconductors, our these results are in qualitative agreement with the major experimental observations of doped cuprates in the SC-state[7,10–15].

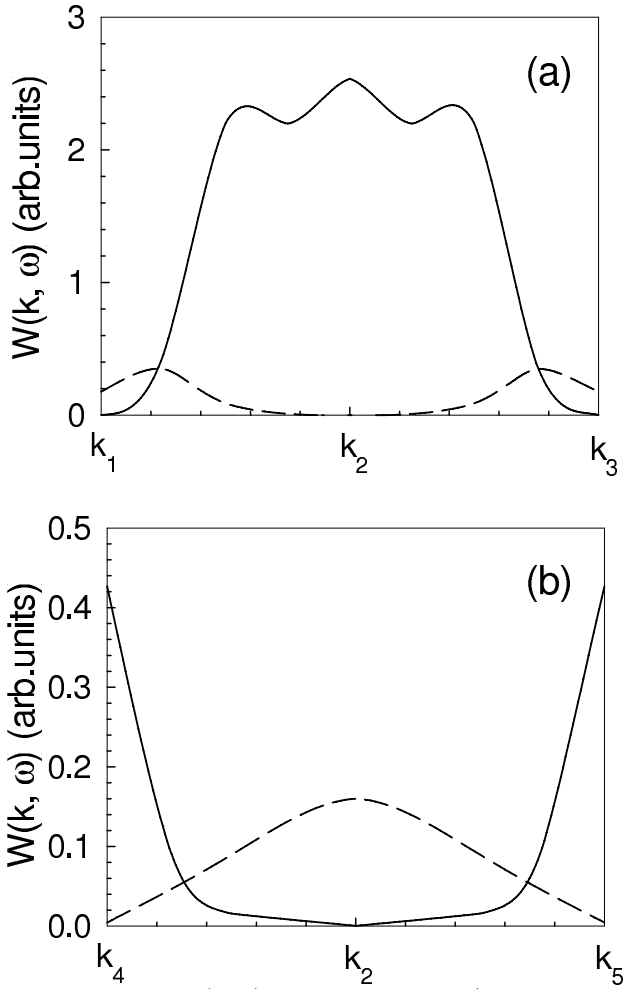

FIG. 7. Function $W(\mathbf{k},\omega)$ in $x_{\rm opt} = 0.18$ for $t/J = 2.5$ with $T = 0.002J$ from (a) $\mathbf{k}_1 = [(1-\delta)/2, 1/2]$ via $\mathbf{k}_2 = [1/2, 1/2]$ to $\mathbf{k}_3 = [(1+\delta)/2, 1/2]$ at $\omega = 0.13J$ (solid line) and $\omega = 0.35J$ (dashed line), and (b) $\mathbf{k}_4 = [(1-\delta')/2, (1-\delta')/2]$ via $\mathbf{k}_2 = [1/2, 1/2]$ to $\mathbf{k}_5 = [(1+\delta')/2, (1+\delta')/2]$ at $\omega = 0.35J$ (solid line) and $\omega = 0.65J$ (dashed line).

The physical interpretation to the above obtained results can be found from the property of the renormalized dressed spin excitation spectrum $\Omega^2_{\mathbf{k}} = \omega^2_{\mathbf{k}} + {\rm Re}\Sigma^{(s)}(\mathbf{k},\Omega_{\mathbf{k}})$ in Eq. (23). Since both MF dressed spin excitation spectrum $\omega_{\mathbf{k}}$ and dressed spin self-energy function $\Sigma^{(s)}(\mathbf{k},\omega)$ in Eq. (22) are strong doping and energy dependent, this leads to that the renormalized dressed spin excitation spectrum also is strong doping and energy dependent. The dynamical spin structure factor in Eq. (23) has a well-defined resonance character, where $S(\mathbf{k},\omega)$ exhibits peaks when the incoming neutron energy ω is equal to the renormalized spin excitation, i.e.,

$$W(\mathbf{k}_c,\omega) \equiv [\omega^2 - \omega^2_{\mathbf{k}_c} - B_{\mathbf{k}_c}{\rm Re}\Sigma^{(s)}(\mathbf{k}_c,\omega)]^2 = [\omega^2 - \Omega^2_{\mathbf{k}_c}]^2 \sim 0, \quad (24)$$

for certain critical wave vectors $\mathbf{k}_c = \mathbf{k}^{(L)}_c$ at low energy, $\mathbf{k}_c = \mathbf{k}^{(I)}_c$ at intermediate energy, and $\mathbf{k}_c = \mathbf{k}^{(H)}_c$ at high energy, then the weight of these peaks is dominated by the inverse of the imaginary part of the dressed spin self-energy $1/{\rm Im}\Sigma^{(s)}(\mathbf{k}^{(L)}_c,\omega)$ at low energy, $1/{\rm Im}\Sigma^{(s)}(\mathbf{k}^{(I)}_c,\omega)$ at intermediate energy, and $1/{\rm Im}\Sigma^{(s)}(\mathbf{k}^{(H)}_c,\omega)$ at high energy, respectively. In the normal-state[18,38], the dressed holon energy spectrum has one branch $\xi_{\mathbf{k}}$, while in the present SC-state, the dressed holon quasiparticle spectrum has two branches $\pm E_{\mathbf{k}}$, this leads to that the dressed spin self-energy function $\Sigma^{(s)}(\mathbf{k},\omega)$ in Eq. (22) is rather complicated, where there are four terms in the right side of Eq. (22). In comparison with the normal-state case[18,38], the contribution for the first and second terms in the right side of the dressed spin self-energy (22) comes from the lower band $-E_{\mathbf{k}}$ of the dressed holon quasiparticle spectrum like the normal-state case, while the contribution for the third and fourth terms in the right side of the dressed spin self-energy (22) comes from the upper band $E_{\mathbf{k}}$ of the dressed holon quasiparticle spectrum. During the above calculation, we find that the mode which opens downward and gives the IC magnetic scattering at low energy is mainly determined by the first and second terms in the right side of the dressed spin self-energy (22), while the mode which opens upward and gives the IC magnetic scattering at high energy is essentially dominated by the third and fourth terms in the right side of the dressed spin self-energy (22), then two modes meet at the commensurate $[1/2, 1/2]$ resonance at intermediate energy. This means that within the framework of the kinetic energy driven superconductivity, as a result of self-consistent motion of the dressed holon pairs and spins, the IC magnetic scattering at both low and high energies and commensurate resonance at intermediate energy are developed. This reflects that the low and high energy spin excitations

drift away from the AF wave vector, or the zero point of $W(\mathbf{k}_c,\omega)$ is shifted from $[1/2,1/2]$ to $\mathbf{k}_c=\mathbf{k}_c^{(L)}$ at low energy and $\mathbf{k}_c=\mathbf{k}_c^{(H)}$ at high energy. With increasing energy from low energy or decreasing energy from high energy, the spin excitations move towards to $[1/2,1/2]$, i.e., the zero point of $W(\mathbf{k}_c,\omega)$ in $\mathbf{k}_c=\mathbf{k}_c^{(L)}$ at low energy or $\mathbf{k}_c=\mathbf{k}_c^{(H)}$ at high energy turns back to $[1/2,1/2]$, then the commensurate $[1/2,1/2]$ resonance appears at intermediate energy. To show this point clearly, the function $W(\mathbf{k},\omega)$ in $x_{\rm opt}=0.18$ for $t/J=2.5$ with $T=0.002J$ from (a) $\mathbf{k}_1=[(1-\delta)/2,1/2]$ via $\mathbf{k}_2=[1/2,1/2]$ to $\mathbf{k}_3=[(1+\delta)/2,1/2]$ at $\omega=0.13J$ (solid line) and $\omega=0.35J$ (dashed line), and (b) $\mathbf{k}_4=[(1-\delta')/2,(1-\delta')/2]$ via $\mathbf{k}_2=[1/2,1/2]$ to $\mathbf{k}_5=[(1+\delta')/2,(1+\delta')/2]$ at $\omega=0.35J$ (solid line) and $\omega=0.65J$ (dashed line) is plotted in Fig. 7, where there is a strong angular dependence with actual minima in $[(1-\delta)/2,1/2]$ and $[1/2,(1-\delta)/2]$, $[1/2,1/2]$, and $[(1-\delta')/2,(1-\delta')/2]$ and $[(1+\delta')/2,(1+\delta')/2]$ for low, intermediate, and high energies, respectively. These are exactly positions of the IC peaks at both low and high energies and resonance peak at intermediate energy determined by the dispersion of very well defined renormalized spin excitations. Since the essential physics is dominated by the dressed spin self-energy renormalization due to the dressed holon bubble in the dressed holon particle-particle channel, then in this sense the mobile dressed holon pairs (then the electron Cooper pairs) are the key factor leading to the IC magnetic scattering peaks at both low and high energies and commensurate resonance peak at intermediate energy, i.e., the mechanism of the IC magnetic scattering and commensurate resonance in the SC-state is most likely related to the motion of the dressed holon pairs (then the electron Cooper pairs). This is why the position of the IC magnetic scattering peaks and commensurate resonance peak in the SC-state can be determined in the present study within the t-J model under the kinetic energy driven SC mechanism, while the dressed spin energy dependence is ascribed purely to the self-energy effects which arise from the the dressed holon bubble in the dressed holon particle-particle channel. Our present result in the SC-state and the previous result in the normal-state[18,38] show that the IC magnetic scattering at low energy appears in both SC- and normal-states, this indicates that the IC magnetic scattering at low energy is not associated with the SC-state, which is similar to stripe models[14,40–42], where the IC magnetic scattering at low energy is due to the formation of magnetic domain lines[14,40–42]. Since the commensurate $[1/2,1/2]$ resonance at intermediate energy and IC magnetic scattering at high energy are absent from the normal-state[18,38], then our present result also show that the commensurate $[1/2,1/2]$ resonance at intermediate energy and IC magnetic scattering at high energy are closely related to the SC-state, which is different from the stripe theory[14,41,42], where the linear spin wave models based the stripe ground state predict that the spin excitations at high energy are nearly symmetric around $[1/2,1/2]$ position and disperse almost linearly with energy[14,41,42], then the commensurate $[1/2,1/2]$ resonance may represent a characteristic energy defined by the size of a stripe domain. Although there are some subtle differences between our present approach and stripe theory, both theories can give the qualitative interpretation for all main features of the unusual spin response of cuprate superconductors[7,10–15].

IV. SUMMARY AND DISCUSSIONS

In summary, within the framework of the kinetic energy driven superconductivity[17], we have discussed the magnetic nature of cuprate superconductors. It is shown that the SC-state is controlled by both SC gap function and quasiparticle coherent weight. This quasiparticle coherent weight is closely related to the dressed holon self-energy from the dressed spin pair bubble, and grows linearly with the hole doping concentration in the underdoped and optimally doped regimes, and then decreases with doping in the overdoped regime, which leads to that the maximal SC transition temperature $T_c^{(d)}$ occurs around the optimal doping $x_{\rm opt}\approx 0.18$, and then decreases in both underdoped and overdoped regimes, in qualitative agreement with the experiments[5]. Although the symmetry of the SC-state is doping dependent, the SC-state has the d-wave symmetry in a wide range of doping. Within this d-wave SC-state, we have calculated the dynamical spin structure factor of cuprate superconductors in terms of the collective mode in the dressed holon particle-particle channel, and reproduce all main features of inelastic neutron scattering experiments in the SC-state[7,10–15], including the energy dependence of the IC magnetic scattering peaks at both low and high energies and commensurate resonance peak at intermediate energy. In particular, we have shown that the unusual IC magnetic excitations at high energy have energies greater than the dressed holon pairing energy (then SC Cooper pairing energy), and are present at the SC transition temperature.

The t-J model is characterized by a competition between the kinetic energy (t) and magnetic energy (J). The magnetic energy J favors the magnetic order for spins, while the kinetic energy t favors delocalization of holes and tends to destroy the magnetic order. Therefore the introduction of the additional second neighbor hopping t' in the t-J model may be equivalent to increase the kinetic energy, and this t' term does not change spin configuration because of the same sublattice hopping. In this case, we[43] have discussed the effect of the additional second neighbor hopping t' on superconductivity within the t-t'-J model, and found that the d-wave SC pairing correlation is enhanced, while the s-wave SC pairing correlation is heavily suppressed.

Superconductivity in cuprates emerges when charge carriers, holes or electrons, are doped into Mott

insulators[4,44]. Both hole-doped and electron-doped cuprate superconductors have the layered structure of the square lattice of the CuO_2 plane separated by insulating layers[4,44]. In particular, the symmetry of the SC order parameter is common in both case[30,45], manifesting that two systems have similar underlying SC mechanism. On the other hand, the strong electron correlation is common for both hole-doped and electron-doped cuprates, then it is possible that superconductivity in electron-doped cuprates is also driven by the kinetic energy as in hole-doped case. Within the t-t'-J model, we[46] have discussed this issue, and found that superconductivity appears around the optimal doping in electron-doped cuprates, and the maximum achievable SC transition temperature is lower than hole-doped cuprates due to the electron-hole asymmetry.

ACKNOWLEDGMENTS

The author would like to thank Dr. Ying Liang, Dr. Bin Liu, Dr. Jihong Qin, Professor Y.J. Wang, and Professor H.H. Wen for the helpful discussions. This work was supported by the National Natural Science Foundation of China under Grant Nos. 10125415 and 90403005.

[1] P.W. Anderson, Science **235**, 1196 (1987).
[2] P.W. Anderson, Phys. Rev. Lett. **67**, 2092 (1991); Science **288**, 480 (2000); Physica C **341-348**, 9 (2000); cond-mat/0108522.
[3] R.B. Laughlin, Phys. Rev. Lett. **79**, 1726 (1997); J. Low. Tem. Phys. **99**, 443 (1995).
[4] See, e.g., M.A. Kastner, R.J. Birgeneau, G. Shiran, and Y. Endoh, Rev. Mod. Phys. **70**, 897 (1998).
[5] See, e.g., J.L. Tallon, J.W. Loram, J.R. Cooper, C. Panagopoulos, and C. Bernhard, Phys. Rev. B **68**, 180501 (2003).
[6] H. Ding, J.R. Engelbrecht, Z. Wang, J.C. Campuzano, S.C. Wang, H.B. Yang, R. Rogan, T. Takahashi, K. Kadowaki, and D.G. Hinks, Phys. Rev. Lett. **87**, 227001 (2001); R.H. He, D.L. Feng, H. Eisaki, J.-I. Shimoyama, K. Kishio, and G.D. Gu, Phys. Rev. B **69**, 220502 (2004).
[7] P. Dai, H.A. Mook, R.D. Hunt, and F. Doğan, Phys. Rev. B**63**, 54525 (2001); H. He, P. Bourges, Y. Sidis, C. Ulrich, L.P. Regnault, S. Pailhés, N.S. Berzigiarova, N.N. Kolesnikov, and B. Keimer, Science **295**, 1045 (2002); N.B. Christensen, D.F. McMorrow, H.M. Rønnow, B. Lake, S.M. Hayden, G. Aeppli, T.G. Perring, M. Mangkorntong, N. Nohara, and H. Tagaki, Phys. Rev. Lett. **93**, 147002 (2004).
[8] K. Yamada, C.H. Lee, K. Kurahashi, J. Wada, S. Wakimoto, S. Ueki, H. Kimura, Y. Endoh, S. Hosoya, and G. Shirane, Phys. Rev. B **57**, 6165 (1998).
[9] S. Wakimoto, H. Zhang, K. Yamada, I. Swainson, H. Kim, and R.J. Birgeneau, Phys. Rev. Lett. **92**, 217004 (2004); M. Fujita, K. Yamada, H. Hiraka, P.M. Gehring, S.H. Lee, S. Wakimoto, and G. Shirane, Phys. Rev. B **65**, 064505 (2002); S. Wakimoto, G. Shirane, Y. Endoh, K, Hirota, S. Ueki, Y.S. Lee, P.M. Gehring, and S.H. Lee, Phys. Rev. B **60**, R769 (1999).
[10] P. Bourges, B. Keimer, S. Pailhés, L.P. Regnault, Y. Sidis, and C. Ulrich, Physica C **424**, 45 (2005); H. He, Y. Sidis, P. Bourges, G.D. Gu, A. Ivanov, N. Koshizuka, B. Liang, C.T. Lin, L.P. Regnault, E. Schoenherr, and B. Keimer, Phys. Rev. Lett. **86**, 1610 (2001).
[11] P. Bourges, Y. Sidis, H.F. Fong, L.P. Regnault, J. Bossy, A. Ivanov, and B. Keimer, Science **288**, 1234 (2000).
[12] M. Arai, T. Nishijima, Y. Endoh, T. Egami, S. Tajima, K. Tomimoto, Y. Shiohara, M. Takahashi, A. Garret, and S.M. Bennington, Phys. Rev. Lett. **83**, 608 (1999).
[13] S.M. Hayden, H.A. Mook, P. Dai, T.G. Perring, and F. Doğan, Science **429**, 531 (2004).
[14] C. Stock, W.J. Buyers, R.A. Cowley, P.S. Clegg, R. Coldea, C.D. Frost, R. Liang, D. Peets, D. Bonn, W.N. Hardy, and R.J. Birgeneau, Phys. Rev. B**71**, 24522 (2005).
[15] J.M. Tranquada, H. Woo, T.G. Perring, H. Goka, G.D. Gu, G. Xu, M. Fujita, and K. Yamada, Nature **429**, 534 (2004); J.M. Tranquada, cond-mat/0512115.
[16] V. Hinkov, S. Pailhés, P. Bourges, Y. Sidis, A. Ivanov, A. Kulakov, C.T. Lin, D.P. Chen, C. Bernhard, and B. Keimer, Science **430**, 650 (2004).
[17] Shiping Feng, Phys. Rev. B **68**, 184501 (2003).
[18] Shiping Feng, Jihong Qin, and Tianxing Ma, J. Phys. Condens. Matter **16**, 343 (2004); Shiping Feng, Tianxing Ma, and Jihong Qin, Mod. Phys. Lett. B**17**, 361 (2003).
[19] Tianxing Ma, Huaiming Guo, and Shiping Feng, Mod. Phys. Lett. B**18**, 895 (2004).
[20] G.M. Eliashberg, Sov. Phys. JETP **11**, 696 (1960); D.J. Scalapino, J.R. Schrieffer, and J.W. Wilkins, Phys. Rev. **148**, 263 (1966).
[21] See, e.g., G.D. Mahan, *Many Particle Physics*, (Plenum Press, New York, 1981), Chapter 9.
[22] Z.X. Shen, D.S. Dessau, B.O. Wells, D.M. King, W.E. Spicer, A.J. Arko, D. Marshall, L.W. Lombardo, A. Kapitulnik, P. Dickinson, S. Doniach, J. DiCarlo, T. Loeser, and C.H. Park, Phys. Rev. Lett. **70**, 1553 (1993); H. Ding, M.R. Norman, J.C. Campuzano, M. Randeria, A.F. Bellman, T. Yokoya, T. Takahashi, T. Mochiku, and K. Kadowaki, Phys. Rev. B**54**, R9678 (1996).
[23] Shiping Feng and Yun Song, Phys. Rev. B **55**, 642 (1997).
[24] J. Kondo and K. Yamaji, Prog. Theor. Phys. **47**, 807 (1972).
[25] Shiping Feng and Zhongbing Huang, Phys. Lett. A **232**, 293 (1997); Feng Yuan, Jihong Qin, Shiping Feng, and W.Y. Chen, Phys. Rev. B **67**, 134505 (2003).
[26] Huaiming Guo and Shiping Feng, cond-mat/0509508.
[27] Z.X. Shen and D.S. Dessau, Phys. Rep. **253**, 2 (1985).
[28] P. Chaudhari and S.Y. Lin, Phys. Rev. Lett. **72**, 1084 (1994); D.H. Wu, J. Mao, S.N. Mao, J.L. Peng, X.X. Xi, T. Venkatesan, R.L. Greene, and S.M. Anlage, Phys. Rev. Lett. **70**, 85 (1993); S.M. Anlage, B.W. Langley, G. Deutscher, J. Halbritter, and M.R. Beasley, Phys. Rev. B **44**, 9764 (1991).
[29] J.A. Martindale, S.E. Barrett, K.E. ÓHara, C.P. Slichter, W.C. Lee, and D.M. Ginsberg, Phys. Rev. B **47**, 9155

(1993); W.N. Hardy, D.A. Bonn, D.C. Morgan, R. Liang, and K. Zhang, Phys. Rev. Lett. **70**, 3999 (1994); D.A. Wollman, D.J. Van Harlingen, W.C. Lee, D.M. Ginsberg, and A.J. Leggett, Phys. Rev. Lett. **71**, 2134 (1993).

[30] See, e.g., C.C. Tsuei and J.R. Kirtley, Rev. Mod. Phys. **72**, 969 (2000).

[31] E. Dagotto and J. Riera, Phys. Rev. B **46**, 12084 (1992); R.T. Scalettar, Physica C **162-164**, 313 (1989); R.T. Scalettar, S.R. White, D.J. Scalapino, and R. Sugar, Phys. Rev. B **44**, 770 (1991); M. Capone, M. Fabrizio, C. Castellani, and T. Tosatti, Science **296**, 2364 (2002).

[32] H.H. Wen, H.P. Yang, S.L. Li, X.H. Zeng, A.A. Soukiassian, W.D. Si, and X.X. Xi, Europhys. Lett. **64**, 790 (2003).

[33] N.-C. Yeh, C.T. Chen, G. Hammerl, J. Mannhart, A. Schmehl, C.W. Schneider, R.R. Schulz, S. Tajima, K. Yoshida, D. Garrigus, and M. Strasik, Phys. Rev. Lett. **87**, 087003 (2001); G. Deutscher, Nature **397**, 410 (1999).

[34] A. Biswas, P. Fournier, M.M. Qazilbash, V.N. Smolyaninova, H. Balci, and R.L. Greene, Phys. Rev. Lett. **88**, 207004 (2002).

[35] C.C. Tsuei, J.R. Kirtley, G. Hammerl, J. Mannhart, H. Raffy, and Z.Z. Li, Phys. Rev. Lett. **93**, 187004 (2004).

[36] Y.J. Uemura, G.M. Luke, B.J. Sternlieb, J.H. Brewer, J.F. Carolan, W.N. Hardy, R. Kadono, J.R. Kempton, R.F. Kiefl, S.R. Kreitzman, P. Mulhern, T.M. Riseman, D.L. Williams, B.X. Yang, S. Uchida, H. Takagi, J. Gopalakrishnan, A.W. Sleight, M.A. Subramanian, C.L. Chien, M.Z. Cieplak, G. Xiao, V.Y. Lee, B.W. Statt, C.E. Stronach, W.J. Kossler, and X.H. Yu, Phys. Rev. Lett. **62**, 2317 (1989); Y.J. Uemura, L.P. Le, G.M. Luke, B.J. Sternlieb, W.D. Wu, J.H. Brewer, T.M. Riseman, C.L. Seaman, M.B. Maple, M. Ishikawa, D.G. Hinks, J.D. Jorgensen, G. Saito, and H. Yamochi, Phys. Rev. Lett. **66**, 2665 (1991).

[37] Y. DeWilde, N. Miyakawa, P. Guptasarma, M. Iavarone, L. Ozyuzer, J.F. Zasadzinski, P. Romano, D.G. Hinks, C. Kendziora, G.W. Crabtree, and K.E. Gray, Phys. Rev. Lett. **80**, 153 (1998).

[38] Shiping Feng and Zhongbing Huang, Phys. Rev. B **57**, 10328 (1998); Feng Yuan et al., Phys. Rev. B **64**, 224505 (2001).

[39] S. Shamoto, M. Sato, J.M. Tranquada, B.J. Sternlib, and G. Shirane, Phys. Rev. B **48**, 13817 (1993).

[40] J. Zaanen and O. Gunnarsson, Phys. Rev. B **40**, 7391 (1989); D. Poilblanc and T.M. Rice, Phys. Rev. B **39**, 9749 (1989).

[41] E.W. Carlson, D.X. Yao, and D.K. Campbell, Phys. Rev. B **70**, 064505 (2004); C.D. Batista, G. Ortiz, and A.V. Balatsky, Phys. Rev. B **64**, 172508 (2001).

[42] F. Krüger and S. Scheidl, Phys. Rev. B **67**, 134512 (2003).

[43] Shiping Feng and Tianxing Ma, Phys. Lett. A, to be published, cond-mat/0506114.

[44] Y. Tokura, H. Takagi, and S. Uchida, Nature **337**, 345 (1989); L. Alff, Y. Krockenberger, B. Welter, M. Schonecke, R. Gross, D. Manske, and M. Naito, Nature **422**, 698 (2003).

[45] C.C. Tsuei and J.R. Kirtley, Phys. Rev. Lett. **85**, 182 (2000).

[46] Tianxing Ma and Shiping Feng, Phys. Lett. A**339**, 131 (2005).